

THE PENNSYLVANIA STATE UNIVERSITY
SCHREYER HONORS COLLEGE

SCHOOL OF ENGINEERING

FORMING AND SPRINGBACK ANALYSIS OF HYBRID MATERIALS

ELIZABETH MARIE MAMROS
FALL 2018

A thesis
submitted in partial fulfillment
of the requirements
for a baccalaureate degree in Mechanical Engineering
with honors in Mechanical Engineering

Reviewed and approved* by the following:

Dr. Chetan Nikhare
Associate Professor of Mechanical Engineering
Thesis Supervisor

Dr. Yi (Elisa) Wu
Chair, Associate Professor of Mechanical Engineering
Honors Adviser

* Signatures are on file in the Schreyer Honors College.

ABSTRACT

Various industries, particularly automotive and aerospace, are continuing to grow their businesses and are seeking ways to improve their manufacturing processes. Some preliminary research has been conducted concerning the use of hybrid materials as a solution, but further analysis is required before these materials can be rolled out into industry universally. Two major benefits of potentially swapping out metal parts for hybrid (metal and composite) components are light weighting and cost reduction, which are two major goals of these industries. It is imperative to understand the properties of the materials used in each manufacturing process as these properties will determine the result of each operation and eventually, the final product. A number of components are manufactured with sheet metal forming processes, and a common unwarranted effect is springback. Springback occurs when the die is removed following a forming operation, and the deformed part transforms its shape as a result of the elastic material properties. A component affected by springback may negatively affect future manufacturing processes, such as incorrect alignment for assembly. To further investigate a solution to this manufacturing defect, trilayer hybrid materials with metal and composite layers are considered. Trilayer sample compositions will be either composite metal composite or metal composite metal sandwiches. Several methodologies and techniques for the layup process are developed, and adjustments are made to resolve sample delamination. Springback data is gathered from channel bend testing. The layup techniques under consideration are resin plus hardener, a pillow method, and an enhanced adhesive mixture. The results from these experiments will support the movement to bring hybrid materials into manufacturing environments and demonstrate the potential benefits of utilizing new layup techniques in the material creation process.

TABLE OF CONTENTS

LIST OF FIGURES	iii
LIST OF TABLES.....	iv
ACKNOWLEDGEMENTS	v
Chapter 1 Introduction.....	1
Chapter 2 Experimental Methodology.....	3
2.1 Layup Process.....	3
Resin Plus Hardener Adhesive.....	4
Pillow Method	4
Enhanced Adhesive with JB weld.....	5
2.2 Tensile Test	5
2.3 Channel Bend Test.....	6
2.4 Springback Measurement.....	7
Chapter 3 Results and Discussion	8
3.1 Layup Process.....	8
3.2 Tensile Test	8
3.3 Channel Bend Test.....	14
3.4 Springback Measurement.....	21
Chapter 4 Conclusions	22
Chapter 5 Future Work	23
BIBLIOGRAPHY	24

LIST OF FIGURES

Figure 1: Hybrid Material Specimen for Channel Bend Test [12].....	4
Figure 2: Pillow Specimen for Channel Bend Test [12].....	4
Figure 3: Dogbone Specimen and Tensile Test Setup on MTS Machine [13].	6
Figure 4: Channel Bend Test Setup on Tinius-Olsen [12].....	6
Figure 5: Springback Measurement [11].	7
Figure 6: Stress-Strain Curves for Metal Specimens [11].	9
Figure 7: Stress-Strain Curves for Composite Specimens [11].	9
Figure 8: Stress-Strain Curves for MCM Specimens [11].....	10
Figure 9: Stress-Strain Curves for CMC Specimens [11].....	10
Figure 10: Stress-Strain Curves for MCMJB Specimens [12].....	11
Figure 11: Stress-Strain Curves for CMCJB Specimens [12].....	11
Figure 12: Stress-Strain Curves for All Specimen Types [11,12].....	12
Figure 13: Fractured Tensile Specimens: (a) CMC, (b) MCM, (c) M, (d) CC [11].....	13
Figure 14: Fractured Tensile Specimens: (a) MCMJB, (b) CMCJB [12].....	13
Figure 15: Force Displacement Curves for M, CMC, and MCM Specimens [11].	15
Figure 16: Force Displacement Curves for CMC Specimens [12].	15
Figure 17: Force Displacement Curves for MCM Specimens [12].....	16
Figure 18: Force Displacement Curves for CC Specimens [12].....	16
Figure 19: Force Displacement Curves for CMC Specimens [12].	17
Figure 20: Force Displacement Curves for CMCJB Specimens [12].	17
Figure 21: Force Displacement Curves for MCMJB Specimens [12].....	18
Figure 22: Force Displacement Curves for CCJB Specimens [12].....	18
Figure 23: Force Displacement Curves for all Compositions [12].	19
Figure 24: Channel Bend Specimens: (a) CMC, (b) MCM, (c) M [11].	19

Figure 25: Channel Bend Specimens: (a) MCM-JB, (b) MCM [12].....	20
Figure 26: Channel Bend Specimens (a) CMC-JB, (b) CMCP, (c) CMC [12].....	20
Figure 27: Channel Bend Specimens: CC and CC-JB [12]......	20

LIST OF TABLES

Table 1: Sample Sets For Testing [12].....	5
Table 2: Mechanical Properties of AA2024, CC, MCMJB, MCM, CMCJB, and CMC Materials [11,12].....	14
Table 3: Springback Half Angles by Sample [11,12].....	21
Table 4: Average Springback Half Angles by Sample [11,12].....	21

ACKNOWLEDGEMENTS

The author would like to thank Penn State Behrend for the support and funding of undergraduate research projects. Special acknowledgment of the following individuals is necessary for their continuous support during this journey.

- Dr. Chetan Nikhare: research supervisor, thesis supervisor
- Dr. Adam Hollinger: honors advisor
- Dr. Yi (Elisa) Wu: honors advisor, faculty reader
- Mr. Glenn Craig: materials/research technician

Chapter 1

Introduction

Billions of metal components are produced each year through various manufacturing methods across the globe, and a number of these are utilized in automotive and aerospace applications. However, these metal components contribute significant masses that negatively affect several factors, such as fuel economy and overall vehicle weights, directly interfering with the leading goals of these industries. In the interest of cost-savings and complying with the increasing number of governmental regulations, manufacturers are searching for innovative methods and materials that will deliver the required strength with a reduction in weight as compared to the current all-metal components. Using less material to form comparable parts will cause a major reduction in strength that can only be combatted by the use of higher strength, higher cost materials. Thus, a material with the appropriate strength value and a decreased gage area is what industry leaders are searching for [1]. Two major considerations when selecting a material for sheet metal processing specifically are strength-to-weight and stiffness-to-weight ratios [2].

Instead of resorting to high strength materials, hybrid materials, including trilayers, are being researched as possibilities for manufacturers. The first obstacle in considering multi-layer materials is designing appropriate layup techniques to create them. One researcher used P2-etch and FPL-etch aluminum surface treatments and discovered that the FPL-etch layup process increased the bonding of the aluminum and carbon fiber layers as well as the fracture toughness six-fold [3]. Another experiment showed that a metal composite metal sandwich caused increased stiffness and resistance to denting when undergoing tooling at low pressures while heating. This technique uses electromagnetic heating of the tool and compression to adhere the layers together [4].

Several studies have shown promising results for bilayer metal-composite materials in increasing fatigue life and impact strength, some of which are already in place in small aerospace and defense

operations. However, these materials are only in use for low-volume components due to the increased manufacturing time required. These experiments also have shown a reduction in springback following processing [5]. Springback is directly related to the elasticity of the material being processed and occurs after a load is removed from the material. This springback effect causes the material to deform in an attempt to return to its previous shape which can be problematic for subsequent operations and tolerance constraints [6].

With the goals of light weighting and reducing the resultant springback angle as dictated by industry, further research is required focusing on layup techniques and material properties. One researcher looked at unidirectional, angle ply, cross ply, and quasi-isotropic layups [7]. A research center is investigating material modeling processes that would include failure. The four failure types under consideration are fiber failure, matrix cracking, buckling, and delamination [8]. Another experiment looking at the layup process found 12 key parameters that are related to the in-plane coordinates for different thicknesses [9]. It is understood that hybrid materials cannot eradicate the springback effect but will be able to reduce the resultant angle [10].

A literature review of the published research concerning hybrid multilayer materials, particularly their resultant springback, shows that this area has not yet been thoroughly investigated. This paper continues the investigation in this area by focusing on the methodology of the layup process and analysis of the springback effect after channel bending [11]. Composite sandwiches comprised of AA 2024 metal and a twill weave carbon fiber were created using various layup techniques including resin with hardener adhesive, a pillow method, and an enhanced adhesive with JB Weld [12]. Specimens of each composition were channel bended, and the springback result was compared to the desired shape. Force displacement curves were constructed from the bending process. Conclusions about layup techniques to decrease delamination and using trilayer hybrid materials to reduce the springback effect in manufacturing are stated.

Chapter 2

Experimental Methodology

An overview of the procedures for the layup process, tensile test, channel bend test, and springback measurements are outlined in this section. The different specimen types under investigation were as follows: composite metal composite (CMC) sandwich, metal composite metal (MCM) sandwich, metal (M) strip, and carbon fiber with resin (CC).

2.1 Layup Process

In these studies [11, 12], two materials were considered: aluminum alloy AA2024 and 2x2 twill weave carbon fiber. Three different layup techniques were utilized to create trilayer hybrid specimens: resin plus hardener, carbon fiber pillow (P), and resin plus hardener and JB weld (JB). Figure 1 shows the configuration of the finished hybrid material specimens, where the two outer layers are of the same material, and the middle layer is the other material. For this investigation, CMC and MCM sandwiches were created. For the metal layers, a sheet of AA2024 was sheared along the rolling direction into strips with dimensions of 152.4 mm (6 inches) in length and 12.5 mm (0.5 inches) in width. The carbon fiber layers were placed at a 90° angle to the rolling direction. The adhesive mixture was brushed onto the surfaces of joining, and then the subsequent layers were added. A uniform weight was applied on top of the samples to create a constant pressure for 24 hours during curing. After curing, the samples were sheared to size for channel bending and also into strips for the CNC to create the dogbones for tensile testing.

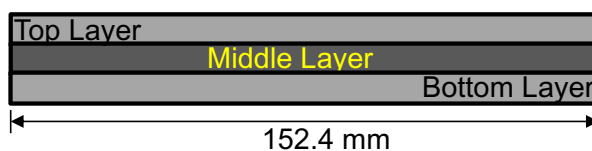


Figure 1: Hybrid Material Specimen for Channel Bend Test [12].

Resin Plus Hardener Adhesive

For the initial set of channel bend specimens, CMC and MCM sandwiches were created using the layup process described above with a 3:1 ratio medium epoxy hardener adhesive. The metal layers were sanded evenly in the rolling direction prior to applying the adhesive to create an increased surface area for bonding. The second set of channel bend specimens also included additional CMC and MCM sandwiches utilizing the same layup process.

Pillow Method

One new layup technique investigated for creating the CMC samples is the pillow method. The resin plus hardener adhesive is used, and this process is very similar to the one outlined above. The key difference for this technique is that the carbon fiber outer layers are wider and longer than the metal strip sandwiched between them allowing for a 3.2 mm (1/8 inch) perimeter overlap of carbon fiber adhered to carbon fiber. The metal layers were also sanded in the rolling direction prior to the material layup for this process.



Figure 2: Pillow Specimen for Channel Bend Test [12].

Enhanced Adhesive with JB weld

A second new layup technique was investigated for creating MCM samples using an enhanced adhesive compound containing JB Weld. To create the adhesive for this technique, a 3:1 ratio medium epoxy hardener mixture was created, and then approximately 5 grams of JB Weld compound (2.5 grams of each component) was blended into the mixture. The key difference for this technique is the different composition used to create the adhesive mixture. The metal strips were sanded perpendicular to the rolling direction to create an increased surface area for bonding. The rest of the layup process for this technique is as described above.

Thus, a total of 39 specimens were tested under channel bending, and their designations by material and adhesive compositions are given in Table 1.

Table 1: Sample Sets For Testing [12].

<i>Composition</i>	<i>Adhesive Compound</i>
MCM	With resin and hardener only
CMC	With resin and hardener only
CC	With resin and hardener only
MCM-JB	With resin, hardener and JB weld
CMC-JB	With resin, hardener and JB weld
CC-JB	With resin, hardener and JB weld
CMC-Pillow	With resin and hardener only

2.2 Tensile Test

Dogbone specimens for the tensile tests were machined using a computer numerical control (CNC) machine so that the rolling direction runs parallel to the length, and the dimensions (A = 9.5 mm; B = 6.35 mm; C = 38.1 mm; and D = 29.7 mm) are shown in Figure 3. The specimens were tested on a MTS machine at 5mm/min using the setup shown in Figure 3. Two small bands of reflective tape were attached at the endpoints of the gage length in order to be captured by the MTS Systems LX Laser Extensometer for increased measurement accuracy. Specimens of the following compositions were tested: composite (CC), metal (M), MCM, CMC, MCM-JB, and CMC-JB.

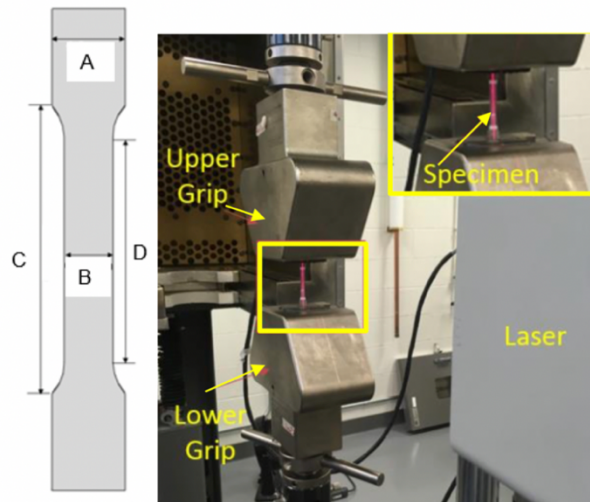


Figure 3: Dogbone Specimen and Tensile Test Setup on MTS Machine [13].

2.3 Channel Bend Test

Each of the aforementioned specimen compositions were channel bend tested using a 120-kip Tinius-Olsen machine to capture the springback effect. Figure 4 depicts the test setup including a square punch and a die with a square cut-out supported on blocks. Specimen placement was consistent for all tests.

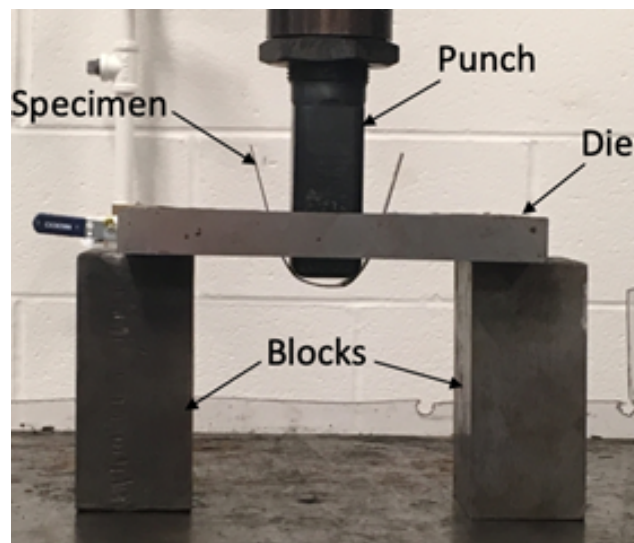


Figure 4: Channel Bend Test Setup on Tinius-Olsen [12].

2.4 Springback Measurement

To measure the springback of the channel bend specimens, the wall angle (θ) shown in Figure 5 was calculated using Equations 1 and 2. Equation 1 uses one of the trigonometric relationships of triangles where x and y are the measured lengths of the horizontal and vertical legs, opposite and adjacent respectively, to the desired angle. The left- and right- side wall angles were averaged to determine the analysis half-angle for the entire specimen. The desired springback half angle (θ_2) is 7.734° based on a die clearance of 3.175 mm with respect to the punch.

$$\theta_1 = \tan^{-1}\left(\frac{x}{y}\right) \quad (1)$$

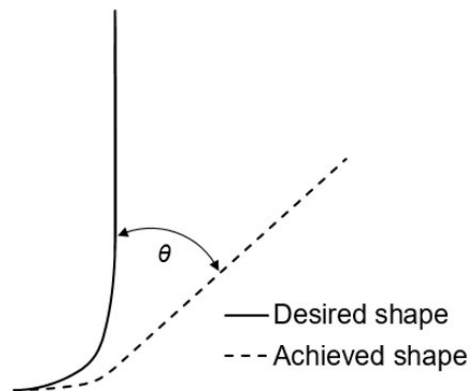


Figure 5: Springback Measurement [11].

Combining the result of Equation 1 and the calculated desired springback angle, the actual springback angle (θ) can be calculated using Equation 2 where θ_1 is the analysis half angle, and θ_2 is the desired springback half angle.

$$\theta = \theta_1 - \theta_2 \quad (2)$$

Chapter 3

Results and Discussion

This section outlines the experimental results and their significance in studying hybrid materials. Results were collected from the layup process techniques, tensile tests, channel bend tests, and springback measurements.

3.1 Layup Process

Each member of the initial set of experiments created with the resin plus hardener adhesive (except for one MCM specimen) experienced delamination during the channel bend test. This delamination made it evident that novel layup techniques were needed to solve this issue. Various parameters that may affect the adhesion between the layers include the amount of adhesive applied to the samples and the composition of the adhesive used for the layup process. The pillow method and enhanced adhesive layup processes proved effective in limiting the number of delaminated samples as shown by the second set of hybrid specimens.

3.2 Tensile Test

Figure 6 shows the stress-strain curve for the metal specimens. Out of all of the specimen types tested, the metal specimens showed the least variability among experiments. The failure strain values range from approximately 0.11 to 0.119 mm/mm.

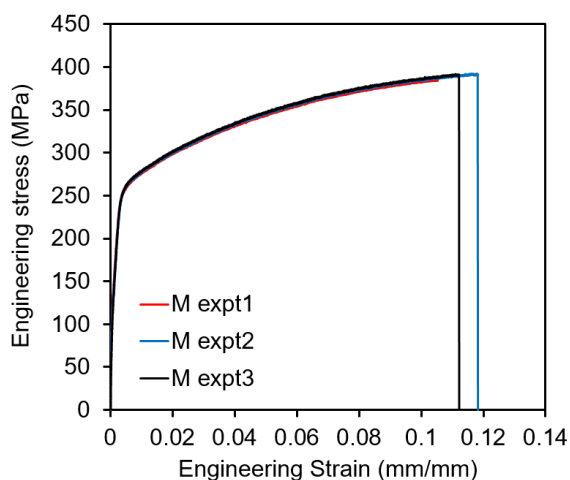


Figure 6: Stress-Strain Curves for Metal Specimens [11].

Figure 7 shows the stress-strain curve for the composite specimens. The stress-strain curves appear nearly linear until failure due to the brittleness of the material. The failure point of the composite specimens averages approximately 30 MPa above the failure point of the metal specimens.

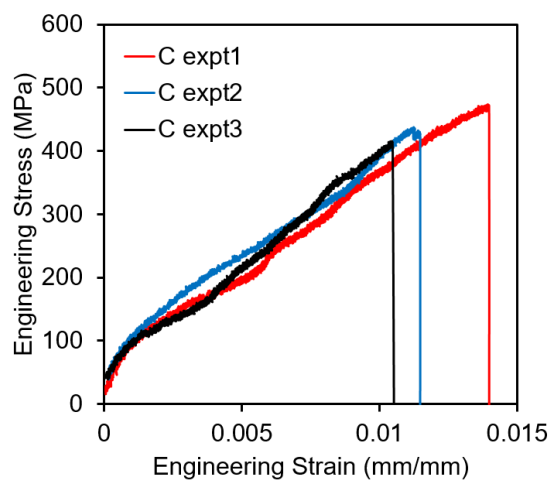


Figure 7: Stress-Strain Curves for Composite Specimens [11].

Figure 8 shows the stress-strain curves for the MCM specimens. The spike in the curves occurs at a strain value of approximately 0.009 mm/mm where the composite layer failed prior to the metal layers failing. The composite layer is behaving similar to a brittle material, while the metal layers appear to be more ductile and failing at higher stress values. For each test, the composite layer on the specimen after failure was shorter in length than the metal layers as expected with the difference in ductility between the two materials. Comparing the lengths of the layers of the failed specimens to an as received specimen

proved that both the metal and composite layers showed elongation after testing, but the metal layers showed a greater percentage of elongation.

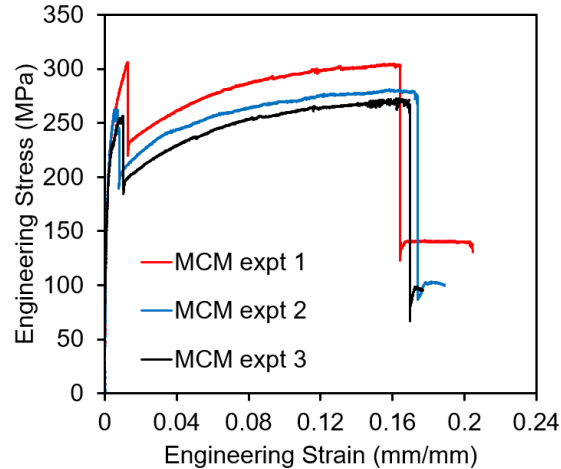


Figure 8: Stress-Strain Curves for MCM Specimens [11].

Figure 9 shows the stress-strain curve for the CMC specimens. The spike in stress occurs where the composite layers failed prior to the metal layer failing. The UTS of the metal layer (disregarding the spike) is approximately 73% of the UTS of the two metal layers together in the MCM experiments. Similar to the MCM results, the metal layer on each specimen after failure appeared to be longer than the composite layers despite the fact that all of the layers were the same length prior to testing.

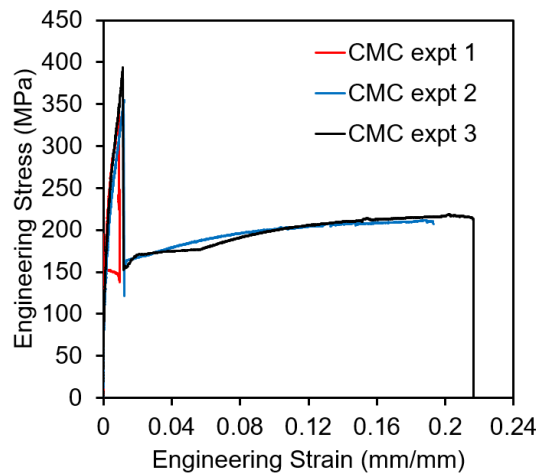


Figure 9: Stress-Strain Curves for CMC Specimens [11].

Figure 10 shows the stress-strain curves for the MCM-JB specimens. Both samples yielded at a strain value of approximately 0.011 mm/mm. The sharp spike at the beginning of the stress-strain curves can be attributed to failure of the composite layer prior to the metal layers.

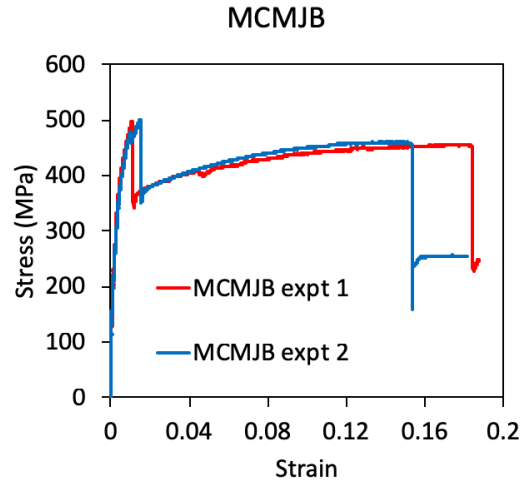


Figure 10: Stress-Strain Curves for MCMJB Specimens [12].

Figure 11 shows the stress-strain curves for the CMC-JB specimens. A sharp decrease in stress by approximately 230 MPa can be observed immediately after the yield point at 0.013 mm/mm. This creates the spike shown in the figure which is expected because the composite layers surrounding the metal will fail prior to the middle metal layer during the tensile test.

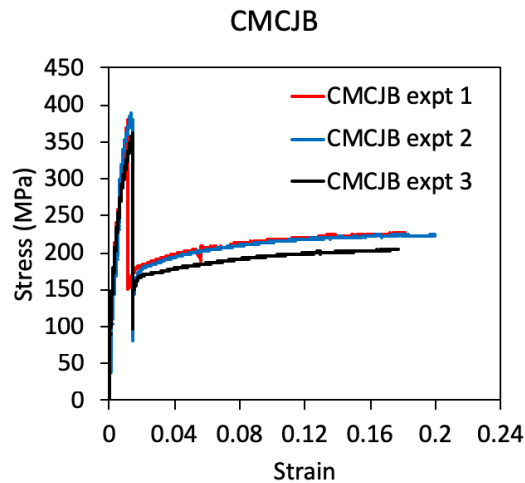


Figure 11: Stress-Strain Curves for CMCJB Specimens [12].

Figure 12 shows the stress-strain curves for the following specimen compositions: MCMJB, MCM, CMC, CMC-JB, M, and CC. Dogbones were not created for the CMC-P and CC-JB specimen compositions

because these results are expected to be similar to the CMC and CC specimen data, respectively. Due to the enhanced adhesive used for creating the CC-JB specimens, the maximum force value is expected to be larger than that of CC. The MCM-JB specimens had the highest yield strength around 500 MPa, followed by CC with 475 MPa, then CMC-JB with 380 MPa, then CMC with 350 MPa, then M with 300Pa, and lastly, MCM with approximately 250 MPa. All specimen compositions yielded between 0 mm/mm and 0.15 mm/mm. MCM-JB showed the largest UTS of approximately 460 MPa. The MCM-JB stress-strain curve exhibits approximately 175 MPa greater stress than the MCM curve. The CMC-JB stress strain curve also experiences slightly higher stress values than its CMC counterpart. This is expected because the enhanced adhesive used to create the JB specimens should increase their tensile strength. The MCM and MCMJB specimens failed at higher stress values than the CMC and CMCJB specimens as expected due to their increased strength from the additional metal layer in their sandwich compositions.

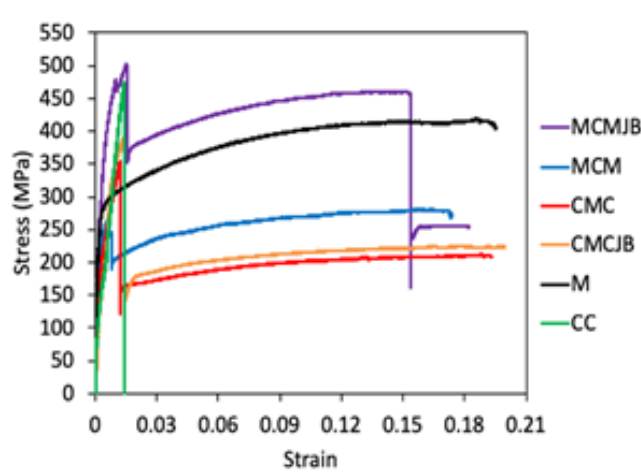


Figure 12: Stress-Strain Curves for All Specimen Types [11,12].

Figure 13 shows the fractured dogbone specimens of types CMC, MCM, M, and CC. For the trilayer specimens, the combination of composite and metal layers contribute different strengths and elasticities to each specimen type causing these specimen compositions to fail at differing stress and strain values accordingly. The CC specimens were not permanently deformed during tested and maintained their as received length as shown in the figure.

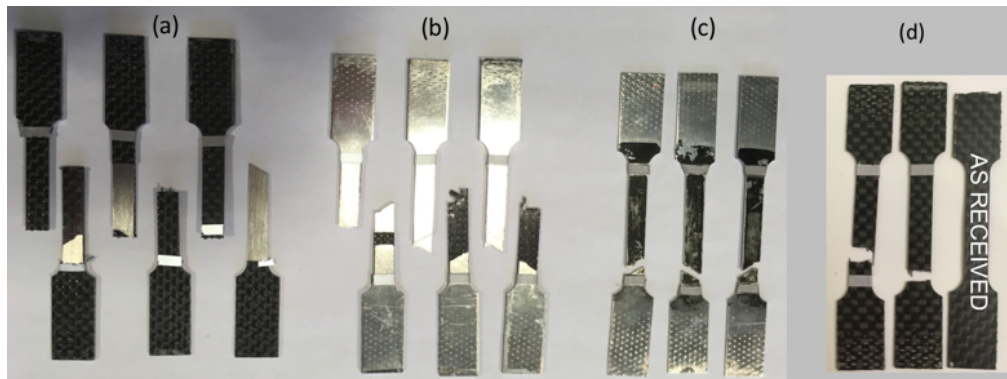


Figure 13: Fractured Tensile Specimens: (a) CMC, (b) MCM, (c) M, (d) CC [11].

Figure 14 shows the fractured tensile specimens for the MCM-JB and CMC-JB compositions. As expected, the metal layers are fragmented at nearly 45° angles, and all of the specimens fractured within the gage length.

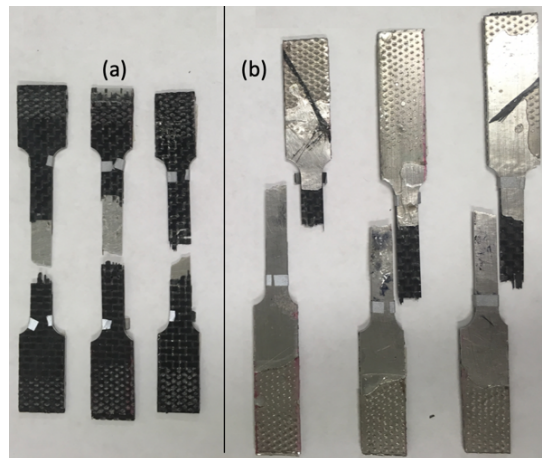


Figure 14: Fractured Tensile Specimens: (a) MCMJB, (b) CMCJB [12].

Table 2 below lists the mechanical properties of AA 2024 (single layer), CC, MCMJB, MCM, CMCJB, and CMC materials collected from the tensile tests and fitting the Holloman Ludwik (power law) equation to the stress-strain curves. Equation 3 is shown below where E is Young's modulus, and for MCM and CMC samples, this value is calculated from the derived Equation 2 (in the textbook) based on statistically indeterminate axially loaded members [14]. E_1 and E_2 are the Young's modulus values of materials 1 and 2, and A_1 and A_2 are the projected areas of materials 1 and 2. YS is the yield strength, and K and n are components of the power law given in Equation 4.

$$E = \frac{E_1 A_1 + E_2 A_2}{A_1 + A_2} \quad (3)$$

$$\sigma = K \cdot \epsilon^n \quad (4)$$

Table 2: Mechanical Properties of AA2024, CC, MCMJB, MCM, CMCJB, and CMC Materials [11,12].

<i>Material</i>	<i>Density (g/cm³)</i>	<i>E (MPa)</i>	<i>YS (MPa)</i>	<i>K (MPa)</i>	<i>n</i>
AA 2024	2.70	72000	271	752	0.26
CC	0.97	32800	464	--	--
MCM-JB	--	61740	507	755	0.18
MCM	--	61740	263	455	0.18
CMC-JB	--	49014	390	370	0.19
CMC	--	49014	356	370	0.22

AA 2024 has a Young's modulus value more than double that of the carbon fiber material. The MCM-JB and CMC-JB materials have increased yield strengths in comparison to the MCM and CMC materials, respectively. This difference is expected due to the enhanced adhesive compound used in the layup process for MCM-JB and CMC-JB. The CMC material resulted in a larger yield strength than the MCM material by approximately 93 MPa.

3.3 Channel Bend Test

Figure 15 displays the force displacement curves for M, CMC, and MCM specimens resulting from the initial round of channel bend testing. The noise evident in the data is most likely due to the specimen overcoming the friction between the specimen and the die as the punch is applying a force to the center of the channel specimen.

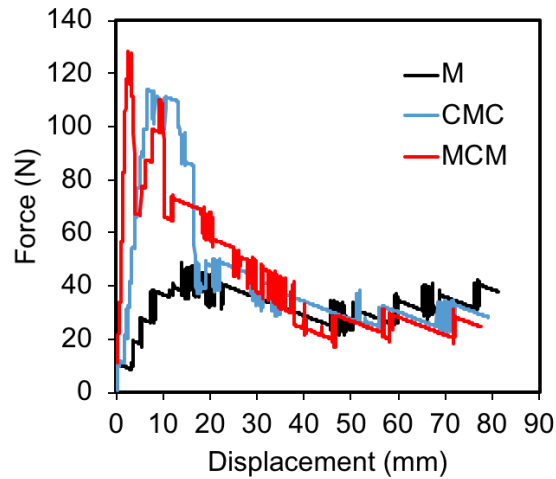


Figure 15: Force Displacement Curves for M, CMC, and MCM Specimens [11].

MCM and CMC specimens were recreated in the second set of channel bend specimens and tested to ensure consistency in the adhesive mixture for the epoxy and hardener ingredients across the various specimen compositions.

Figure 16 shows the force displacement curves for the recent CMC specimens. CMC experiment 2 matches most closely to the previous CMC curve shown in Figure 15, but the variation in the data is most likely explained by the delamination of the previous channels during testing.

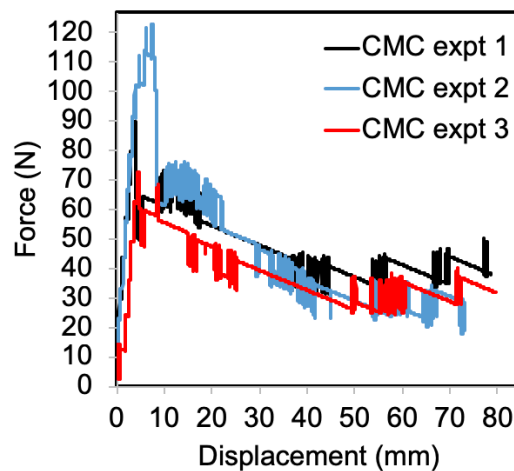


Figure 16: Force Displacement Curves for CMC Specimens [12].

Figure 17 shows the force displacement curves for the recent MCM experiments. The yield strength average of these experiments is approximately 250 N which is more than double the yield strength of the

previous MCM experiments. This difference is most likely due to the MCM specimens not experiencing delamination during the recent round of testing.

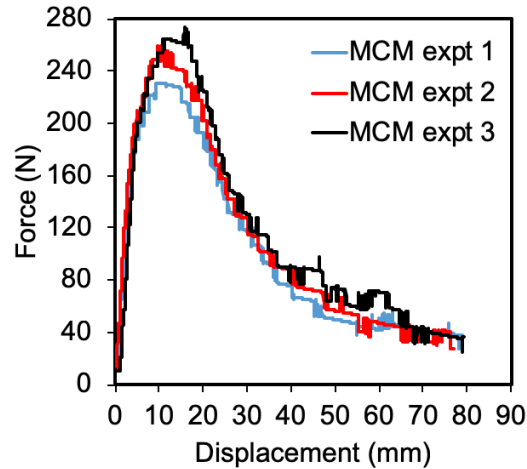


Figure 17: Force Displacement Curves for MCM Specimens [12].

The force displacement curves for CC specimens are shown in Figure 18. The CC specimens failed at relatively low forces under 50 N. This is expected because the carbon fiber layers after the layup process are brittle. Due to its ductility, the CC specimens displaced approximately 8 mm further than the other specimen compositions before reaching the maximum force.

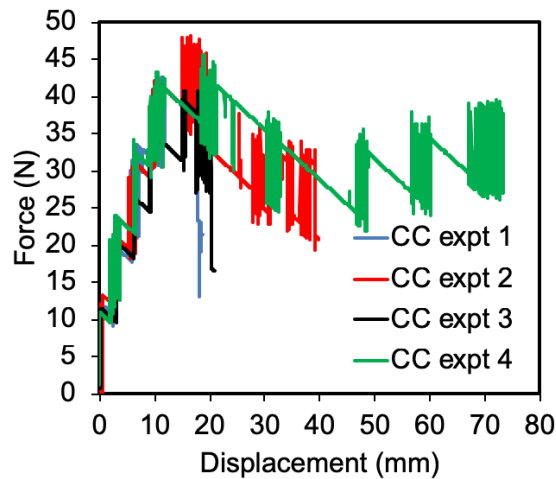


Figure 18: Force Displacement Curves for CC Specimens [12].

Figure 19 displays the force displacement curves for the CMC-P type specimens. All three CMC-P experiments experienced greater maximum force values than the CMC specimens by a margin 20 N or more.

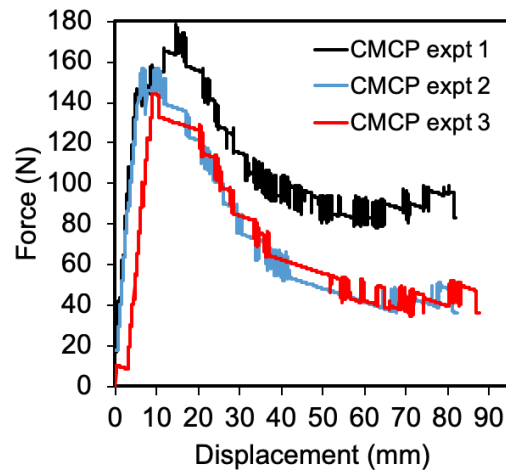


Figure 19: Force Displacement Curves for CMC Specimens [12].

The force displacement curves for the CMC-JB specimens are shown in Figure 20. The average maximum force for the CMC-JB specimens is approximately 20 N lower than the maximum force for the CMC-P specimens but still significantly larger than the maximum force for the CMC specimens.

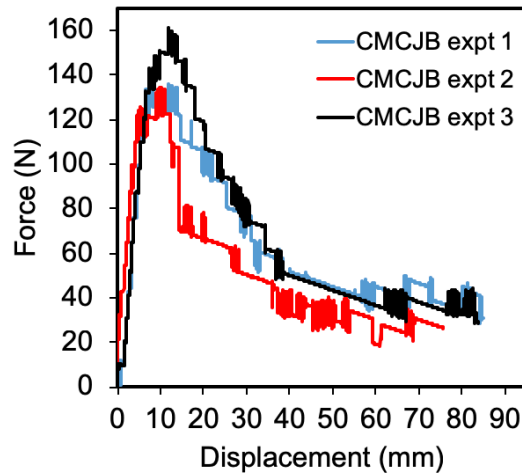


Figure 20: Force Displacement Curves for CMCJB Specimens [12].

Figure 21 shows the force displacement curves for the MCM-JB experiments. This specimen type experienced the largest average force at approximately 285 N.

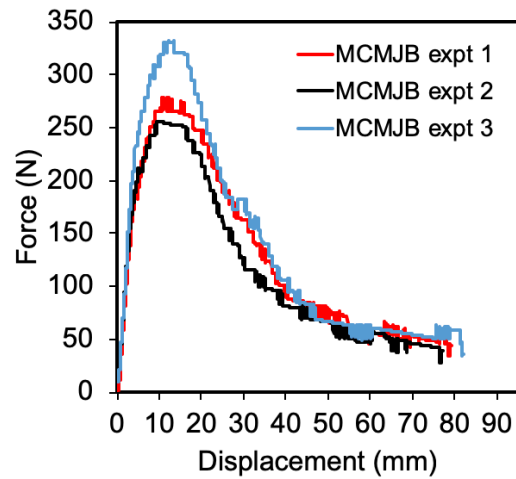


Figure 21: Force Displacement Curves for MCMJB Specimens [12].

The force displacement curves for the CC-JB specimens are displayed in Figure 22. The variation among the curves is the result of some specimens fracturing during testing while others remained intact. As shown by the differences in displacement, two specimens were able to withstand the punch force for over twice the displacement of the fractured specimens. Data collection for these two specimens ended after the channel bend operation was complete, and fracture had not occurred.

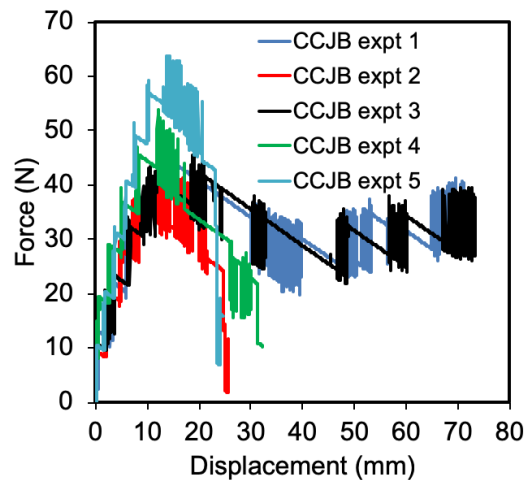


Figure 22: Force Displacement Curves for CCJB Specimens [12].

Figure 23 shows a combination of the force displacement curves for all specimen compositions: CMC-JB, CMC, CMC-P, MCM-JB, MCM, CC-JB, and CC. The curves for the CC-JB and CC specimens lay nearly on top of one another and have the lowest maximum force value of approximately 45 N. The

MCM-JB curve reaches a maximum force slightly above that of the MCM curve. The CMC-P curve sits slightly above the CMC-JB curve in the figure, but the CMC curve shows significantly lower maximum stress values than both the CMC-P and CMC-JB curves.

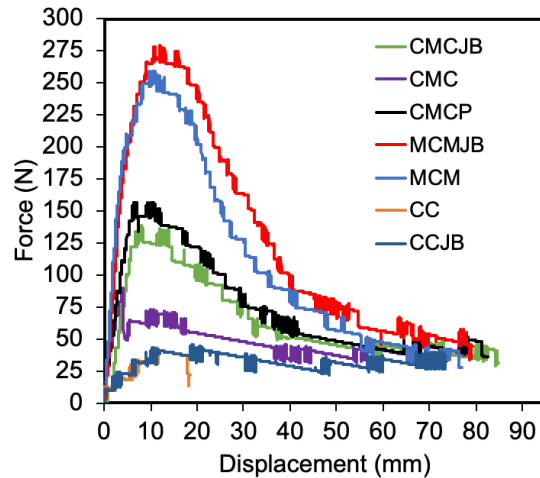


Figure 23: Force Displacement Curves for all Compositions [12].

The deformed channel bend specimens for CMC, MCM, and M compositions from the initial set of specimens are shown in Figure 24 [11]. A sole MCM specimen (the bottom specimen in (b)) did not delaminate during the channel bend test of this initial set. All other MCM and all CMC specimens experienced delamination.

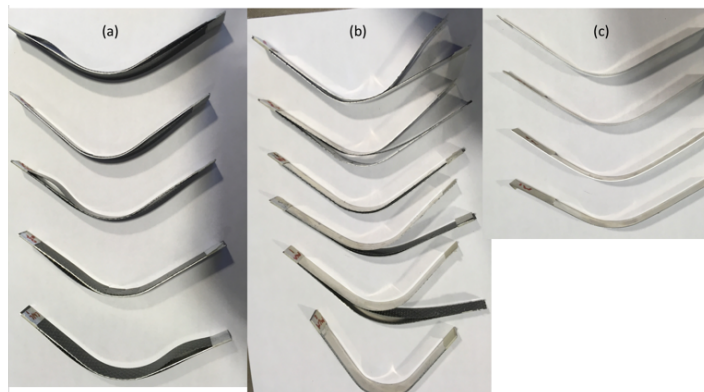


Figure 24: Channel Bend Specimens: (a) CMC, (b) MCM, (c) M [11].

The MCM-JB and recent MCM channel bend specimens are exhibited in Figure 25. Neither of these specimen compositions experienced delamination during the bending process.

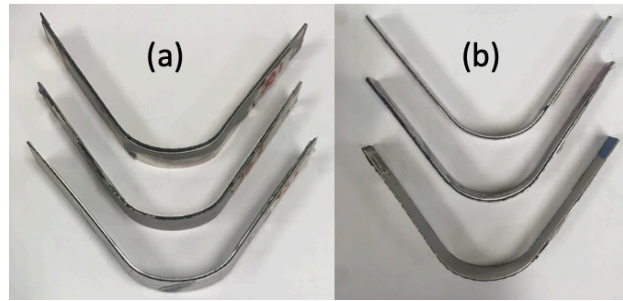


Figure 25: Channel Bend Specimens: (a) MCM-JB, (b) MCM [12].

Figure 26 shows the CMCJB, CMCP, and recent CMC specimens following channel bend testing. One of the CMCJB specimens delaminated as well as all of the CMC specimens. The CMCP specimens were able to undergo the channel bending process without exhibiting delamination.

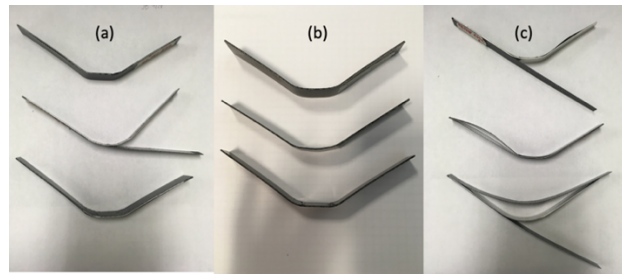


Figure 26: Channel Bend Specimens (a) CMC-JB, (b) CMCP, (c) CMC [12].

The CC and CCJB channel bend specimens are shown in Figure 27. As shown by the top view and also side views of the specimens, the majority of the specimens for these compositions fractured during the bending test as expected since the materials exhibit brittle behavior. However, two of the CCJB specimens remained intact throughout the bending operation and returned to their original flat shapes once released from the die.

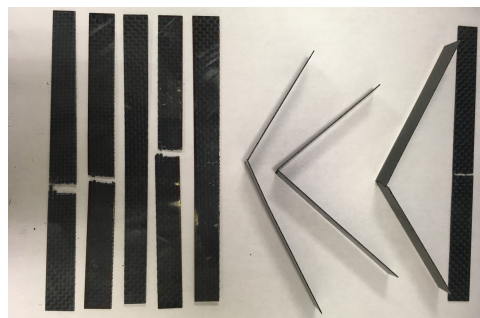


Figure 27: Channel Bend Specimens: CC and CC-JB [12].

3.4 Springback Measurement

Table 3 shows the springback half angles resulting from the channel bend tests for each specimen composition. The second set of specimens, including CMCJB, MCMJB, CMC*, MCM*, and CMCP compositions, showed very consistent half angle results across each specimen type with 5° or less of variation between experiments. The single MCM specimen from the initial set that did not exhibit delamination (Experiment 6) shows a significantly smaller half angle of approximately 20° less than the other previous MCM experiments.

Table 3: Springback Half Angles by Sample [11,12].

<i>Springback Half Angle (°)</i>						
Comp	Expt1	Expt2	Expt3	Expt4	Expt5	Expt6
CMC	42.77	47.67	52.67	38.05	51.42	--
M	48.41	49.27	42.47	50.14	--	--
MCM	55.07	56.43	43.76	47.02	51.32	27.27
CMCJB	47.79	43.09	51.42	--	--	--
MCMJB	27.85	25.53	27.90	--	--	--
CMC*	48.98	49.99	49.12	--	--	--
MCM*	29.87	28.50	29.78	--	--	--
CMCP	47.26	50.24	49.60	--	--	--

Table 4 shows the average springback half angles for all specimen compositions. The CC specimens fractured during testing, but a few of the CC-JB specimens returned to their original 180° shape after the punch force was removed. The CMC-JB, CMC, CMCP, and M specimens had similar average springback half angles ranging between 47° and 50°. This is expected since these four specimen compositions each contain one layer of AA 2024. The MCM-JB and MCM specimens resulted in similar average springback half angles ranging from 27° to 30°.

Table 4: Average Springback Half Angles by Sample [11,12]

<i>Composition</i>	<i>Average Springback Half Angle (°)</i>
M	47.61
CC	fracture
CMC-JB	47.43
CMC	49.36
CMCP	49.03
MCM-JB	27.13
MCM	29.3
CC-JB	82.27

Chapter 4

Conclusions

Innovative layup process techniques to solve the issue of delamination and the use of hybrid materials to reduce the springback angle after material deformation were studied in this investigation. AA 2024 was combined with carbon fiber to create trilayer specimens with CMC and MCM sandwich compositions that were then channel bend tested. These hybrid specimens were measured after forming, and their resulting springback angles were calculated. Three layup process techniques were compared and consisted of resin plus hardener, a pillow method, and an enhanced adhesive compound.

Through this investigation, it was found that the pillow method was effective in eliminating delamination from the CMC specimens, and the enhanced adhesive compound increased the strength as well as reduced the number of delaminated samples for the CMC and MCM compositions. Additionally, the MCMJB specimens showed the greatest reduction in average springback half angle.

Based on these results, metal components could be manufactured with two slightly thinner metallic layers sandwiching a composite layer, reducing the overall weight and potentially the springback half angle as long as delamination does not occur. The incorporation of hybrid materials into manufacturing environments could be extremely beneficial in assisting with light weighting and cost reduction provided that appropriate layup techniques are utilized to create these materials and further testing is completed to ensure their feasibility for the desired application.

Chapter 5

Future Work

Future work will pertain to obtaining additional material properties for these hybrid compositions by performing various tests, such as hardness and fatigue tests. Additional layup process methodologies can be developed to continue combatting delamination and focusing on adhesion between the layers in the hybrid materials. Further investigation is required to determine an appropriate method to convert these manual layup techniques into automated manufacturing processes. Numerical simulations to support experimental results may also be created in the future to be compared with experimental results.

Another focus area that requires further investigation is the use of hybrid materials in high temperature environments. Some manufacturing processes require the use of heat, and the resin plus hardener adhesive used in this work cannot withstand high temperatures. Future studies will need to look into using high temperature adhesives specifically and the change in material properties at various temperatures.

BIBLIOGRAPHY

- [1] Nikhare, C. P., 2017, "Springback Analysis in Bilayer Material Bending; ASME International Mechanical Engineering Congress and Exposition," (58356) pp. V002T02A062.
- [2] Haase, R., Müller, R., Landgrebe, D., 2015, "Process Design for Hybrid Sheet Metal Components," *Acta Metallurgica Sinica (English Letters)*, **28**(12) pp. 1518-1524.
- [3] Lawcock, G., Ye, L., Mai, Y., 1997, "The Effect of Adhesive Bonding between Aluminum and Composite Prepreg on the Mechanical Properties of Carbon-Fiber-Reinforced Metal Laminates," *Composites Science and Technology*, **57**(1) pp. 35-45.
- [4] Asnafi, N., Langstedt, G., Andersson, C. -, 2000, "A New Lightweight Metal-Composite-Metal Panel for Applications in the Automotive and Other Industries," *Thin-Walled Structures*, **36**(4) pp. 289-310.
- [5] Gresham, J., Cantwell, W., Cardew-Hall, M. J., 2006, "Drawing Behaviour of Metal-composite Sandwich Structures," *Composite Structures*, **75**(1) pp. 305-312.
- [6] Yuen, W. Y. D., 1996, "A Generalised Solution for the Prediction of Springback in Laminated Strip," *Journal of Materials Processing Technology*, **61**(3) pp. 254-264.
- [7] Soden, P.D., Hinton, M.J., and Kaddour, A.S., 2004, "Failure Criteria in Fibre-Reinforced-Polymer Composites," Elsevier, Oxford, pp. 30-51.
- [8] Orifici, A. C., Herszberg, I., and Thomson, R. S., 2008, "Review of Methodologies for Composite Material Modelling Incorporating Failure," *Composite Structures*, **86**(1) pp. 194-210.
- [9] Grenestedt, J.L., and Gudmundson, P., 1993, "Optimal Design with Advanced Materials," Elsevier, Oxford, pp. 311-336.
- [10] Jung, W., Chu, W., Ahn, S., 2007, "Measurement and Compensation of Spring-Back of a Hybrid Composite Beam," *Journal of Composite Materials*, **41**(7) pp. 851-864.
- [11] Mamros, E. M., and Nikhare, C. P., 2018, "Springback Analysis in Hybrid Material Deformation," *Proc. IMECE 2018*.
- [12] Mamros, E. M., and Nikhare, C. P., 2018, "Springback Analysis of Hybrid Materials Created Through Alternative Layup Processes," *Proc. MSEC 2019*.
- [13] Mamros, E. M., and Nikhare, C. P., 2018, "Experimental Investigation on Tube Flaring with a Rotational Tool," *Proc. IDDRG 2018*.
- [14] Hibbeler, R. C., 2014, "Mechanics of Materials, 9th edition, Pearson Prentice Hall, NJ, pp. 139.

ACADEMIC VITA

Academic Vita of Elizabeth M. Mamros

ebm5129@gmail.com

www.linkedin.com/in/elizabeth-mamros

EDUCATION

The Pennsylvania State University, Erie PA: 2018

Bachelor of Science in Mechanical Engineering

Minors in Mathematics and Spanish

Schreyer Honors College - Honors in Mechanical Engineering

WORK EXPERIENCE

Ford Motor Company: Manufacturing Engineering Intern

Dearborn, MI: May 2018 – August 2018

- Developed pseudo VIN methodology with team to protect PII during external data transfer
- Derived statistical model to power warranty analysis tool combining WERS and AWS data
- Assisted with data validation, development, and user feedback collection for web dashboard

Penn State Behrend: Undergraduate Researcher

Erie, PA: May 2017 – December 2018

- Presented on analysis of springback effect in trilayer sheet metal forming at IMECE 2018
- Presented on revolutionary tube flaring technique utilizing a rotational tool at IDDRG 2018
- Considered the layup process and developed new techniques for creating hybrid materials
- Investigated the feasibility of integrating trilayer sheet metal into automotive applications
- Focused on cost reduction and decreased shape deformation of sheet metal parts

LORD Corporation: Student Associate in Operational Excellence

Erie, PA: August 2016 – April 2018

- Updated the mold prep standards on 529 SAP routers saving the facility over \$64,000
- Debugged and assisted coding a scheduling database in Visual Studio for HCL sector
- Learned to operate Dot Peener and created a training document with visuals for new operators
- Served as project manager for Adhesive 5S event to reduce downtime and other sources of waste

McDonald's: Shift Manager

McMurray, PA: September 2012 – August 2016

- Oversaw and positioned a diverse crew to ensure a safe and productive shift
- Acquired ability to adapt to dynamic work environment with unforeseen challenges

LEADERSHIP AND ACTIVITIES

Tau Beta Pi – the Engineering Honors Society: PA-M Chapter President

Society of Women Engineers

American Society of Mechanical Engineers

Study Abroad Program in Ronda, Spain